3.3 Bio-kinetics of POEC in tumor-bearing mice

We have already reported that PTD-ODD-β-galactosidase fusion protein was delivered and stabilized in hypoxic regions in tumors after intraperitoneal injection of the fusion protein (14). In present study, we examined if POEC could function as an optical probe specific to tumor hypoxia. Because HeLa/5HRE-Luc cells stably retain a luciferase reporter gene under the control of HIF-1-responsive promoter (17), the existence of hypoxic regions in tumor xenografts was visualized by imaging of hypoxia-responsible expression of luciferase in the tumors (Fig. 4). Cy5.5 fluorescence image was detected in entire bodies within a few minutes after administration of POEC, then the image became thinner and 24 hr after the probe administration, the fluorescent image in the tumors became high contrast compared with their surrounding regions, and reached high magnitude of fluorescence (Fig. 4, upper panels, red cycles). High accumulation of Cy5.5 fluorescence was observed in some specific organs such as kidney, liver, bladder and small intestine. Strong fluorescent signals were observed in the entire area of the back. Although strong fluorescent signal was also observed in the back of non-tumor bearing mice, no fluorescent signal was observed in their hind legs 24 hr after the probe administration (Fig. 4, middle panels). When Cy5.5-EGFP was injected into tumor bearing mice, although some images were also detected in tumors (Fig. 4, lower panels, blue cycles), the image were much smaller and stay shorter than the one of POEC image. The non-specific fluorescent signals of Cy5.5-EGFP in the back were also weaker than that of POEC. The fluorescent signals in the tumors and the back of the mice gradually decreased day by day, but remained until 1 to 2 weeks in detectable magnitude. Now we are examining POE labeling with other NIR dye and obtaining more tumor specific images (much lower background). We are going to confirm the specificity of the probes to hypoxic tumor cells by immuno-histochemical analysis.

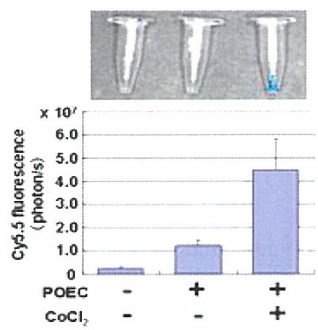

Fig. 3. Analysis of ODD regulation of POEC. The cells were treated with (+) or without (-) POEC as Figure 2 legend. For the hypoxia-mimic treatment, the medium and reagents contained PHD inhibitor ($CoCl_2$). The cells were harvested and analyzed for Cy5.5-fluorescenct intensity by using IVIS200™ imaging system. The experiment was done in triplicate. The representative images are shown in upper panel and average fluorescence intensity of each sample is shown in lower graph.

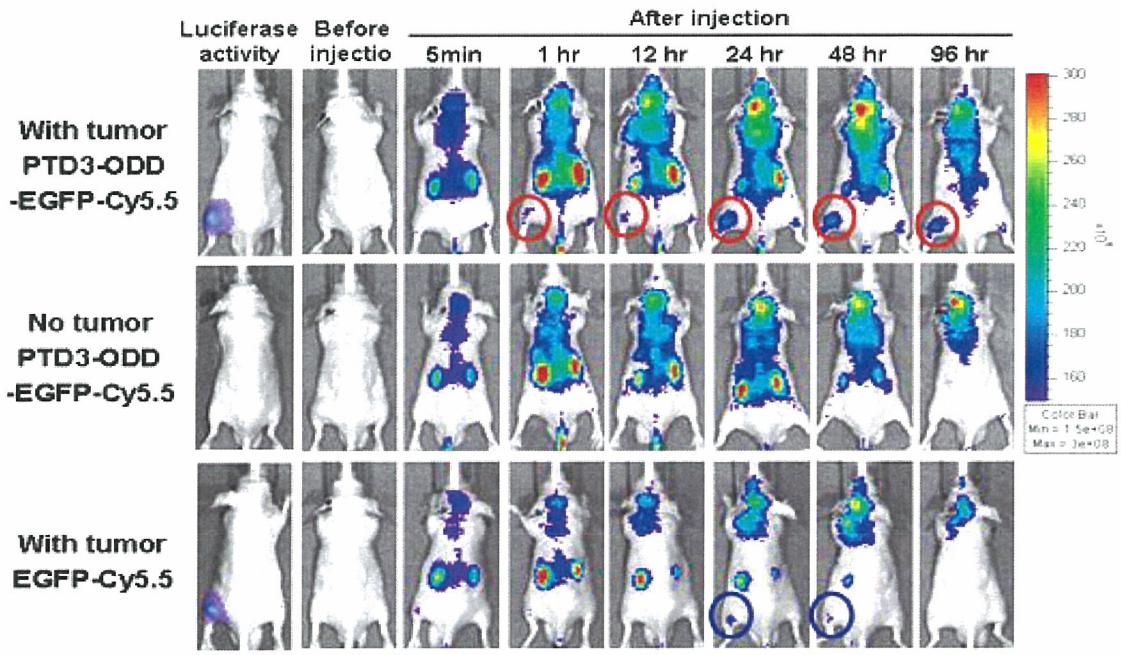

Fig. 4. In vivo fluorescence imaging of POEC. POEC and EGFP-Cy5.5 (1.0 nmol per body) were intravenously injected to tumor-free or tumor-bearing nude mice. Cy5.5 fluorescent signal was detected by IVIS200^{TM} imaging system at the indicated time after probe injection. Image in tumor of POEC (red cycle) and EGFP-Cy5.5 (blue cycle) are shown in figure.

4. CONCLUSION

In this study, we reveal that a PTD-ODD fusion protein has potential to make a unique probe for detecting tumor hypoxia. Because tumor hypoxia is a hallmark of malignancy and poor prognosis, such a probe would open a new avenue in both cancer diagnosis and therapies. At the same time, we can demonstrate that an optical imaging system is a very useful tool to evaluate the specificity of a probe *in vivo*. In our evaluation system, we made the best use of the multiplicity of optical imaging: we visualized the target of tumor hypoxia by bioluminescence imaging using a luciferase reporter vector containing a hypoxia-responsive promoter, and evaluate bio-kinetics of the probe with fluorescence imaging. Such optical imaging systems can accelerate the development of new probes for therapeutic and diagnostic use.

ACKNOWLEDGEMENT

We would like to thank Dr. Kazuhiro Tanabe (Department of Energy and Hydrocarbon Chemistry, Faculty of Engineering, Kyoto university, Kyoto, Japan) for fluorescent spectrometer technical support; Ms. Yumi Takahashi, Akiyo Morinibu and Kazumi Shinomiya for assistance. This study is a part of Kyoto City Collaboration of Regional Entities for the Advancement of Technological Excellence of JST on basis of research results supported in part by grant-in aids for Scientific Researches (A) (No.14205037 and No.15201033).

REFERENCES

1. P. Vaupel, F. Kallinowski and P. Okunieff, "Blood flow, oxygen and nutrient supply, and metabolic microenvironmento of human tumors: a review", Cancer Res. 49 (23), 6449-6465 (1989).
2. Brown JM, Wilson WR. Exploiting tumour hypoxia in cancer treatment. Nat Rev Cancer. 2004 Jun;4(6):437-47.
3. Harris AL. Hypoxia--a key regulatory factor in tumour growth. Nat Rev Cancer. 2002 Jan;2(1):38-47.
4. G. L. Semenza, "Regulation of mammalian O_2 homeostasis by hypoxia-inducible factor 1", Annu. Rev. Cell. Dev. Biol.15, 551-578 (1999).
5. G. L. Semenza, "Targeting HIF-1 for cancer therapy", Nat. Rev. Cancer (3), 721-732 (2003).
6. G. L. Semenza and G. L. Wang, "A nuclear factor induced by hypoxia via de novo protein synthesis binds to the human erythropoietin gene enhancer at a site required for transcriptional activation", Mol. Cell. Biol. 12, 5447-5454 (1992).
7. L. E. Huang, J Gu, M. Schau and H. F. Bunn, "Regulation of hypoxia-inducible factor 1 alpha is mediated by an O2-dependent degradation domain via the ubiquitin-proteasome pathway", Proc. Natl. Acad. Sci. U S A 95, 7987-7992 (1998).
8. R. K. Bruick and S. L. McKnight, "A conserved family of prolyl-4-hydroxylases that modify HIF", Science 294, 1337-1340 (2001).
9. A. C. Epstein, J. M. Gleadle, L. A. McNeill LA, et al., "C. elegans EGL-9 and mammalian homologs define a family of dioxygenases that regulate HIF by prolyl hydroxylation", Cell 107, 43-54 (2001).
10. M. E. Cockman, N. Masson, D. R. Mole, et al., "Hypoxia inducible factor-alpha binding and ubiquitylation by the von Hippel-Lindau tumor suppressor protein", J. Biol. Chem. 275, 25733-25741 (2000).
11. M. Ohh, C. W. Park, M. Ivan, et al., "Ubiquitination of hypoxia-inducible factor requires direct binding to the beta-domain of the von Hippel-Lindau protein", Nat. Cell. Biol. 2, 423-7 (2000).
12. P. J. Kallio, W. J. Wilson, S. O'Brien, Y. Makino and L. Poellinger, "Regulation of the hypoxia-inducible transcription factor 1alpha by the ubiquitin-proteasome pathway", J. Bio.l Chem. 274, 6519-6525 (1999).
13. H. Harada, S. Kizaka-Kondoh, M. Hiraoka. "Mechanism of hypoxia-specific cytotoxicity of procaspase-3 fused with a VHL-mediated protein destrauction motif of HIF-1α containing Pro564". FEBS Lett. 580, 5718-5722 (2006)

14. H. Harada, M. Hiraoka, S. Kizaka-Kondoh. "Antitumor effect of TAT-oxygen-dependent degradation-caspase-3 fusion protein specifically stabilized and activated in hypoxic tumor cells". Cancer Res. 62, 2013-2018 (2002).
15. S. Kizaka-Kondoh, M. I noue, H. Harada, M. Hiraoka. "Tumor hypoxia: A target for selective cancer therapy" Cancer Sci. 94, 1021-1028 (2003)
16. M. Inoue, M. Mukai, Y. Hamanaka, M. Tatsuta, M. Hiraoka, S. Kizaka-Kondoh. "Targeting hypoxic cancer cells with a protein prodrug is effective in experimental malignant ascites" Int J Oncol. 25, 713-720 (2004)
17. H. Harada, S. Kizaka-Kondoh, M. Hiraoka. "Optical imaging of tumor hypoxia and evaluation of efficacy of a hypoxia-targeting drug in living animals" Mol Imaging 4, 182-193 (2005).
18. H. Harada, S. Kizaka-Kondoh, M.Hiraoka "Antitumor protein therapy; application of the protein transduction domain to the development of a protein drug for cancer treatment" Breast Cancer 13, 16-26 (2006).

*e-mail: skondoh@kuhp.kyoto-u.ac.jp; phone: +81-75-751-4242; fax: + 81-75-771-9749

FEBS Letters 580 (2006) 5718–5722

Mechanism of hypoxia-specific cytotoxicity of procaspase-3 fused with a VHL-mediated protein destruction motif of HIF-1α containing Pro564

Hiroshi Harada[a,b], Shinae Kizaka-Kondoh[a,c,*], Masahiro Hiraoka[a]

[a] *Department of Radiation Oncology and Image-applied Therapy, Kyoto University Graduate School of Medicine, 54 Kawahara-cho, Shogoin, Sakyo-ku, Kyoto 606-8507, Japan*
[b] *Nano-Medicine Merger Education Unit, Kyoto University, Japan*
[c] *COE Formation for Genomic Analysis of Disease Model Animals with Multiple Genetic Alterations, Kyoto University Graduate School of Medicine, Japan*

Received 29 July 2006; revised 9 September 2006; accepted 11 September 2006

Available online 22 September 2006

Edited by Veli-Pekka Lehto

Abstract Under normoxic conditions the alpha-subunit of hypoxia-inducible factor (HIF-1α) protein is targeted for degradation by the von Hippel-Lindau (VHL) tumor suppressor protein acting as an E3 ubiquitin ligase. Recently, we developed a hypoxia-targeting protein, TOP3, which consisted of procaspase-3 with the VHL-mediated protein destruction motif of HIF-1α. This design enables procaspase-3 to be regulated similarly with HIF-1α, being degraded under normoxia while stabilized under hypoxia. Furthermore, stabilized TOP3 was cleaved by the hypoxic stress-induced endogenous caspases and thus the procaspase-3 was converted to active caspase-3 specifically under hypoxic conditions. These data demonstrated that the VHL-mediated protein destruction motif of HIF-1α endowed procaspase-3 with hypoxia-specific cytotoxicity.

Keywords: Hypoxia-inducible factor-1; von Hippel-Lindau; Caspase-3; Hypoxia; Apoptosis

1. Introduction

Hypoxia-inducible factor (HIF) is a transcriptional complex that mediates a broad range of cellular and systemic responses to hypoxia [1]. HIF-1 is a heterodimer composed of α and β subunits, and α subunit of HIF-1 (HIF-1α) is regulated in an oxygen-dependent manner at the post-translational level [2–4]. HIF-1α contains oxygen-dependent degradation (ODD) domains, which contains proline residues, proline-402 and proline-564. In normoxia, HIF-1α is hydroxylated at these proline residues by prolyl-4-hydroxylases [5,6]. The modification accelerates the interaction of the HIF-1α protein with the von Hippel-Lindau (VHL) tumor suppressor protein, resulting in the rapid ubiquitination and subsequent degradation of the protein by the 26S proteasome [7–10].

Recently, we screened ODD domain mutants of human HIF-1α protein and determined the $ODD_{548–603}$, which endowed fusion proteins with sufficient oxygen-dependent degradation regulation [11]. In order to specifically eradicate HIF-1α-expressing hypoxic cells in solid tumors, we constructed procaspase-3 fused with $ODD_{548–603}$ and HIV-Tat protein-transduction domain (PTD). The final product was named TOP3 (Tat-ODD-Procaspase-3) [11–14]. The HIV-Tat PTD domain is derived from human immunodeficiency virus type-1 Tat protein and efficiently delivers TOP3 to any tissue in vivo. The procaspase-3 comes from human caspase-3 protein [15] and confers cytocidal activity to TOP3. We already reported that TOP3 had anti-tumor activity in xenografts model with various cancer cells [11–14] and induced apoptosis to hypoxic tumor cells in xenografts [14].

In the present study, we clarify the mechanism of TOP3 activation and confirm its hypoxia-specific cytotoxity.

2. Materials and methods

2.1. Cell culture and hypoxic treatment in vitro

CFPAC-1 and MIA PaCa-2 human pancreatic cancer cell lines, HeLa human cervical epithelial adenocarcinoma cell line, A549 human lung adenocarcinoma cell line, WiDr human colorectal adenocarcinoma cell line and 786-O human renal cell carcinoma cell line were purchased from the American Type Culture Collection. HeLa/EF-Luc and HeLa/5HRE-Luc cell clones were isolated as described previously [14]. WT8, a 786-O cell clone stably transfected with a plasmid coding hemagglutinin (HA)-tagged VHL, was a kind gift from Dr. William G. Kaelin Jr. [16]. CFPAC-1 was maintained as described previously [11], and the other cells were maintained at 37 °C in 5% FBS-Dulbecco's modified Eagle's medium (Nacalai Tesque, Kyoto, Japan) supplemented with penicillin (100 units/ml) and streptomycin (100 μg/ml).

Hypoxic condition of <0.02% of oxygen tension was attained by the use of a Bactron Anaerobic Chamber, BACLITE-1 (Sheldon Manufacturing Inc., Cornelius, OR). Cells were incubated in the chamber for at least 6 h before various treatments.

2.2. Formulation of TOP3 fusion protein

The Tat-ODD-Procaspase-3 fusion protein (TOP3) was prepared and dissolved in 10 mM Tris–HCl buffer (pH 8.0), as described previously [11]. The final concentration of TOP3 preparation was 15 μg/ml for in vitro experiments if not indicated, and 10 mM Tris–HCl (pH 8.0) was used as the buffer in both in vivo and in vitro experiments if not indicated.

2.3. Experimental procedures for analyses of TOP3 activation in vitro

Cells were pre-incubated under aerobic or hypoxic condition for 6 h, added with TOP3, and incubated further for 20 h before analyses.

As for the Western blot analysis, cells were seeded at 1×10^5 cells/well in a 6-well plate, treated as above and the lysates were prepared by suspending cells from each well in 100 μl of 1 × loading buffer. Twenty μl of the lysate was electrophoresed per lane on a 15% (for

*Corresponding author. Fax: +81 75 771 9749.
E-mail address: skondoh@kuhp.kyoto-u.ac.jp (S. Kizaka-Kondoh).

0014-5793/$32.00
doi:10.1016/j.febslet.2006.09.025

TOP3/caspase-3), a 10% (for VHL) or a 7.5% (for HIF-1α) SDS-polyacrylamide gel. TOP3/caspase-3, VHL and HIF-1α were detected by polyclonal anti-caspase-3 antibody (Cell Signaling Technology Inc., Osaka, Japan), monoclonal anti-HA antibody (Roche Diagnostics Japan, Tokyo, Japan) and monoclonal anti-HIF-1α antibody (BD Bioscience Pharmingen, San Diego, CA), respectively. The polyclonal and the monoclonal primary antibodies were then reacted with anti-rabbit and anti-mouse IgG horseradish peroxidase linked antibodies (Amersham Biosciences Corp., Piscataway, NJ), respectively. Detection was carried out with a chemiluminescence-based method using the ECL-PLUS system (Amersham Biosciences Corp.).

As for the DNA fragmentation analysis, genomic DNA was isolated from 6×10^5 cells with Quick Apoptotic Ladder Detection Kit (BioVision Research Products, Mountain View, CA). DNA was electrophoresed in a 1.5% agarose gel.

As for the FACS analysis, the cells were harvested, gently suspended in PBS and mixed with equal volume of 2 × hypotonic fluorochrome solution (100 μg/ml propidium iodide in 0.2% sodium citrate–0.2% Triton X-100) immediately before the analysis with a flow cytometry using CELLQuest (BD Biosciences, Franklin Lakes, NJ).

As for the analysis of caspase-3 after TOP-3 treatment, the cells were seeded at 2×10^4 cells/well in a 24-well plate, pre-incubated for 16 h and treated with TOP3 for 0, 2, 4, 6 or 8 h. As for the analysis of endogenous capsase-3 and -9 activities, similarly seeded cells were cultured with the medium, which was pre-exposed to hypoxic conditions. Then the cells were incubated under hypoxic or aerobic conditions and harvested after indicated time of incubation. Caspase-3 and -9 activities in 50 μl lysates were measured by using Colorimetric Protease Assay Kit according to the manufacturer's instructions (MBL, Nagoya, Japan). The experiments were done in triplicate and the mean of $OD_{405\,nm}$/50 μg was calculated.

3. Results

3.1. Hypoxia-dependent activation of TOP3

We previously showed citocidal effect of TOP3 on hypoxic cells in the xenografts of a human pancreatic cancer cell line [11,14]. TOP3 was designed to be degraded in normoxic cells through the function of ODD domain of human HIF-1α protein which is sensitive to the VHL-mediated destruction in normoxia. The design allows the conversion of the procaspase-3 domain to active caspase-3 under hypoxia, executing apoptotic killing of the cells.

These expectations were tested as follows. Firstly, the stability of TOP3 was compared with that of HIF-1α protein under aerobic and hypoxic conditions (Fig. 1A). CFPAC-1 cells were cultured under aerobic (lanes 1 and 2) and hypoxic (lanes 3 and 4) conditions and the protein levels of TOP3 and HIF-1α were tested with (lanes 2 and 4) or without (lanes 1 and 3) addition

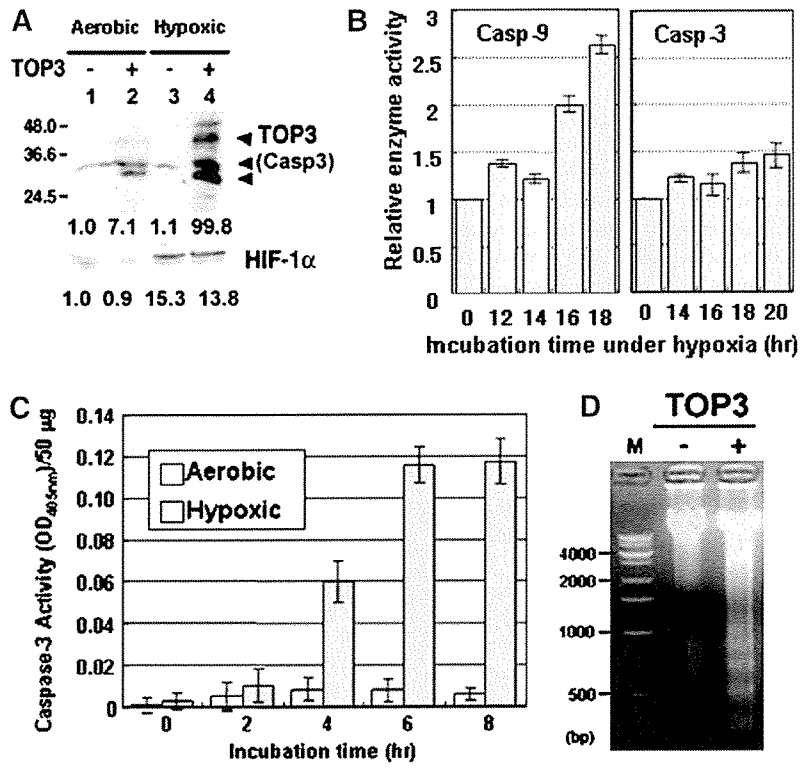

Fig. 1. Hypoxia-dependent stabilization and activation of TOP3 in vitro. (A) CFPAC-1 cells were treated with the buffer only (–; lanes 1 and 3) or TOP3 (+; lanes 2 and 4) under aerobic (lanes 1 and 2) or hypoxic (lanes 3 and 4) conditions for 20 h. TOP3 (upper panel) and HIF-1α (lower panel) proteins in the cells were analyzed by Western blotting with a polyclonal anti-caspase-3 and a monoclonal HIF-1α antibody, respectively. TOP3, its major derivative proteins and endogenous caspase-3 are indicated by arrowheads. The relative density of the bands of TOP3 (upper panel) and HIF-1α (lower panel) proteins of the lanes 2–4 to the lane 1 are indicated below each panel, respectively. (B) CFPAC-1 cells were cultured under hypoxic conditions for indicated period of time and then cell lysates were prepared. Caspase-9 (left) and -3 (right) activities in the cell lysates were measured and relative caspase activities to the 0 h are indicated. (C) CFPAC-1 cells were cultured under aerobic (open bars) and hypoxic (gray bars) conditions for 16 h and then treated with TOP3 or the buffer for the indicated period of time. Total cell lysates were prepared and then $OD_{405\,nm}$ of the lysates was measured. TOP3-derived caspase-3 activity was calculated using the following formula: ($OD_{405\,nm}$/50 μg of the TOP3-treated cells) – ($OD_{405\,nm}$/50 μg of the buffer-treated cells). Results are the means of three independent experiments ± S.D. (D) The cells were treated with the buffer (–) and TOP3 (+) for 20 h under hypoxic conditions. Then the genomic DNA was isolated and analyzed by electrophoresis with a 1.5% agarose gel.

of TOP3. Hypoxic treatment markedly stabilized TOP3 and the protein level was elevated more than 14-fold (Fig. 1A upper panel, lane 2 vs. lane 4). In the same cell preparation, a comparable 14-fold increase was noted for HIF-1α as well (Fig. 1A lower panel, lane 2 vs. lane 4). The control protein without the ODD domain was unaffected by the oxygen tension of the culture (data not shown). These results demonstrate that the stability of TOP3 is sensitive to oxygen concentration as designed.

When CFPAC-1 cells were tested, endogenous caspase-9, the principal caspase in the pathway of mitochondria mediated apoptosis [17], gradually increased and reached the peak after 18 h under hypoxia (Fig. 1B; left panel). However, endogenous caspase-3 activity increased only marginally during the observation period (Fig. 1B; right panel). On the other hand, addition of TOP-3 increased the total caspase-3 activity more than 20-fold when the culture was kept under hypoxia (Fig. 1C). Under this condition, TOP3 induced DNA fragmentation of the cells (Fig. 1D). These results demonstrate that the increase in caspase-3 activity of TOP3-treated cells under hypoxia was due to stabilization and conversion of TOP3 to active caspase-3, resulting in DNA fragmentation. Hypoxia-specific apoptosis induction by TOP3 was also observed other human cancer cell lines such as CFPAC-1, MIA PaCa-2, A549 and WiDr (data not shown), indicating that the function of TOP3 is not cell line-specific.

3.2. VHL-mediated degradation of TOP3

The above observations demonstrate destruction and stabilization of TOP-3 paralleled with those of HIF-1α protein, suggesting that both proteins are under regulation of the VHL mediated degradation system. This was tested by the use of 786-O cells which lacked functional VHL and therefore ubiquitination-mediated degradation through ODD domain does not take place in this cell line. As a positive control, VHL reconstituted WT8 cells were used [16]. In these cells, TOP3 was stabilized if VHL was not expressed (Fig. 2A; upper and lower panels, lane 2) and degraded if VHL was reconstituted (Fig. 2A; upper and lower panels, lane 4). The TOP3 was stabilized (Fig. 2A; upper panel, lanes 6 and 8) and enhanced apoptosis of hypoxic cells (Fig. 2B; lanes 6 and 8) regardless of the VHL status (Fig. 2A; lower panel, lanes 5–8). In contrast, TOP3 did not induce apoptosis regardless of VHL status of the cells as long as the cells were under aerobic conditions (Fig. 2B; lanes 2 and 4).

These results indicate following two. Firstly, the degradation of TOP3 under aerobic conditions is dependent on the VHL function, indicating that it is regulated by the same VHL-mediated protein degradation mechanism as the one of HIF-1α [7–10]. Secondly, the stabilized TOP3 still requires another step to induce apoptosis and this step requires hypoxia.

3.3. Enhancement of hypoxia-induced apoptosis in various cancer cell lines by TOP3

The requirement of hypoxia for the TOP3-induced apoptosis suggests that the cleavage mediated conversion of TOP to caspase-3 is likely to be executed by the endogenous caspases which are activated by hypoxic stress. To assess this possibility, human cancer cell lines, CFPAC-1, MIA PaCa-2, and A549 were treated with TOP3 under hypoxia or normoxia. Morphological observation demonstrated that TOP3 treatment induced cytotoxicity specifically under hypoxia (Fig. 3A). Moreover, FACS analysis confirmed that TOP3 treatment under hypoxic conditions induced degradation of genome DNA as suggested by the increase in the sub-G1 fraction, indicative of the caspase-3 mediated apoptosis of the cells (Fig. 3B). Sub-G1 fraction increased in TOP3 treated CFPAC-1, MIA PaCa-2 and A549 cells under hypoxic conditions by around 10-fold, and were 28.0 ± 2.1%, 27.5 ± 3.8% and 56.5 ± 0.8%, respectively.

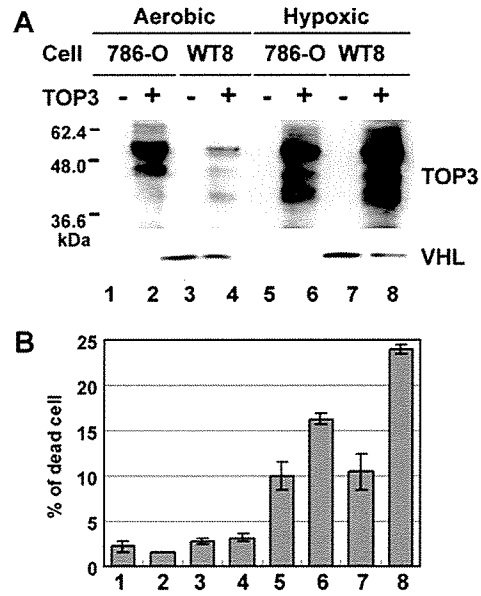

Fig. 2. VHL-dependent ODD regulation of TOP3. 786-O (VHL-deficient renal cell carcinoma cell line) and WT8 (HA-tagged VHL-transfectant clone of 786-O) were treated with the buffer only (−; lanes 1, 3, 5 and 7) or TOP3 (+; lanes 2, 4, 6 and 8) under aerobic (lanes 1–4) or hypoxic (lanes 5–8) conditions. (A) TOP3 (upper panel) and VHL (lower panel) proteins in total cell lysate prepared from each culture were detected by western blot analysis with anti-caspase-3 polyclonal and anti-HA monoclonal antibodies, respectively. (B) DNA contents of these cells were analyzed by flow cytometry and % of population in sub-G1 fraction is indicated as % of dead cell.

4. Discussion

In the present study, we examined the molecular mechanism of activation of procaspase-3 fused with $ODD_{548-603}$, which has VHL-mediated protein destruction motif of HIF-1α containing only 564-proline residue. The results are summarized in Fig. 4.

The ODD domain of HIF-1α including the 564-proline residue physically interacts with VHL which plays a key role in the degradation of the protein through the ubiquitin-proteasome pathway [3–10]. The TOP3 carries the $ODD_{548-603}$ domain and therefore, its ODD regulation was expected to be dependent on VHL expression. Indeed, TOP3 was found to be stable in VHL-deficient 786-O cells even under aerobic conditions (Fig. 2A). These results indicate that TOP3 behaves similarly as HIF-1α and is stabilized in the hypoxic cells in vitro. In our experiments using xenografts, at-ODD-β-galactosidase injected intraperitoneally was specifically detected in the hypoxic regions of tumor xenografts [11]. Present study

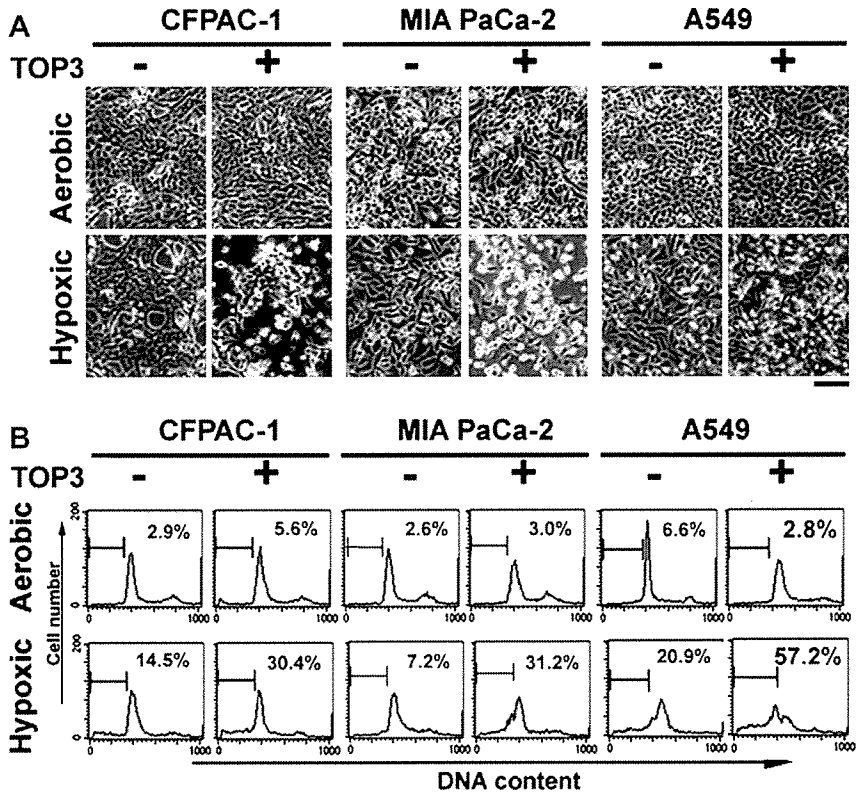

Fig. 3. Enhancement of hypoxia-induced apoptosis by TOP3. CFPAC-1, MIA PaCa-2 and A549 cells were treated with TOP3 (+) or the buffer only (−) for 20 h under aerobic or hypoxic conditions. (A) The morphologies of the cells were observed under an inverted microscope just before FACS analysis. Bar = 200 μm. (B) DNA contents of these cells were analyzed by flow cytometry. % of population in sub-G1 fraction is indicated in each chart. The experiments were done in triplicate and representative photographs (A) and charts (B) are shown.

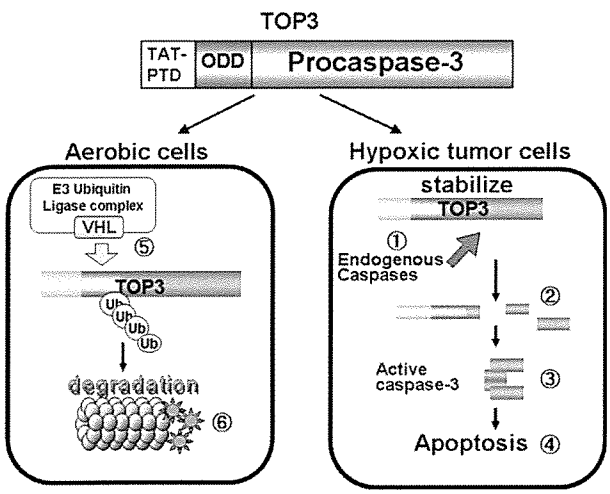

Fig. 4. Mechanism of hypoxia-specific cytotoxicity of TOP3. TOP3 enters in cells by the function of protein transduction domain (PTD) of HIV TAT protein. (1) In hypoxic tumor cells, endogenous caspases are activated to some extent (Fig. 1B). (2) When TOP3 enters in hypoxic tumor cells, TOP3 is cleaved (Fig. 1A, lane 4). (3) Activity of caspase-3 in TOP3-treated hypoxic tumor cells significantly increases (Fig. 1C). (4) DNA fragmentation (Figs. 1D and 3B) is induced and TOP3-treated hypoxic tumor cells undergo apoptosis (Fig. 3). The ODD of TOP3 is the VHL-mediated protein destruction motif of HIF-1α and TOP3 is degraded by VHL-mediated system under normoxia (Fig. 2). (5) When TOP3 enters in aerobic cells, TOP3 is recognized by VHL and (6) degraded through ubiquitin-proteasome system.

confirms that PTD-ODD fusion proteins can be regulated similarly as HIF-1α via VHL-mediated protein destruction motif of HIF-1α in vitro.

Because TOP3 is composed of a dormant form of caspase-3, it has to be cleaved to become active form. That is, stabilization of TOP3 itself cannot induce apoptosis. Indeed, TOP3 was stabilized in 786-O cells under normoxia but did not induce cell death (Fig. 2C). The endogenous caspase activities are brought about by a hypoxic stress (Fig. 1B). Although the major apoptosis pathway induced by hypoxic stress is the mitochondria-mediated 'intrinsic' pathway, in which caspase-9 plays a major role, recent studies suggest the involvement of both the intrinsic and the death receptor-mediated 'extrinsic' pathways in hypoxia-induced apoptosis [18]. TOP3 efficiently enhance the preexisting apoptotic signal leading to more than 20-fold increases of caspase-3 activity (Fig. 1C) and induced DNA fragmentation (Fig. 1D) and cell death (Figs. 2 and 3). All of these characteristics must have contributed not only to the specific targeting of HIF-1α-expressing/hypoxic tumor cells but also to minimizing the obvious side effect to normal tissues in our in vivo experiments [11–14].

It has been reported that hypoxia-induced apoptosis depends on wild-type p53 to a large extent [19–22] and that increased p53 induces apoptosis through a pathway including Apaf-1 and caspase-9 [23]. Thus the extent of hypoxia-induced apoptosis might differ due to p53 status. Interestingly, under hypoxic conditions A549 cells, which possess wild type p53 [24], underwent apoptosis to a larger extent than CFPAC-1

and MIA PaCa-2 cells, which possess mutant type p53 ([25] and Fig. 3).

Acknowledgments: We are grateful to Dr. William G. Kaelin Jr. for 786-O cells and their VHL-expressing clones (WT8); Akiyo Morinibu, Emi Nishimoto, Naoko Murakami-Harada, Yumi Takahashi and Kazumi Shinomiya for skilled technical assistance. This work was supported in part by Grant-in-Aid for Scientific Research on Priority Areas, Cancer, from the Ministry of Education, Culture, Sports, Science and Technology, and by a Grant-in-Aid for the 2nd and 3rd Term Comprehensive 10-Year Strategy for Cancer Control from the Ministry of Health, Labor and Welfare, Japan. This study is a part of joint research, which is focusing on the development of the basis of technology for establishing COE for nano-medicine, carried out through Kyoto City Collaboration of Regional Entities for Advancing Technology Excellence (CREATE) assigned by Japan Science and Technology Agency (JST).

References

[1] Semenza, G.L. (1999) Regulation of mammalian O2 homeostasis by hypoxia-inducible factor 1. Annu. Rev. Cell Dev. Biol. 15, 551–578.
[2] Semenza, G.L. and Wang, G.L. (1992) A nuclear factor induced by hypoxia via de novo protein synthesis binds to the human erythropoietin gene enhancer at a site required for transcriptional activation. Mol. Cell. Biol. 12, 5447–5454.
[3] Huang, L.E., Gu, J., Schau, M. and Bunn, H.F. (1998) Regulation of hypoxia-inducible factor 1 alpha is mediated by an O2-dependent degradation domain via the ubiquitin-proteasome pathway. Proc. Natl. Acad. Sci. USA 5, 7987–7992.
[4] Kallio, P.J., Wilson, W.J., O'Brien, S., Makino, Y. and Poellinger, L. (1999) Regulation of the hypoxia-inducible transcription factor 1alpha by the ubiquitin-proteasome pathway. J. Biol. Chem. 274, 6519–6525.
[5] Bruick, R.K. and McKnight, S.L. (2001) A conserved family of prolyl-4-hydroxylases that modify HIF. Science 294, 1337–1340.
[6] Epstein, A.C., Gleadle, J.M., McNeill, L.A., Hewitson, K.S., O'Rourke, J., Mole, D.R., Mukherji, M., Metzen, E., Wilson, M.I., Dhanda, A., Tian, Y.M., Masson, N., Hamilton, D.L., Jaakkola, P., Barstead, R., Hodgkin, J., Maxwell, P.H., Pugh, C.W., Schofield, C.J. and Ratcliffe, P.J. (2001) *C. elegans* EGL-9 and mammalian homologs define a family of dioxygenases that regulate HIF by prolyl hydroxylation. Cell 107, 43–54.
[7] Cockman, M.E., Masson, N., Mole, D.R., Jaakkola, P., Chang, G.W., Clifford, S.C., Maher, E.R., Pugh, C.W., Ratcliffe, P.J. and Maxwell, P.H. (2000) Hypoxia inducible factor-alpha binding and ubiquitylation by the von Hippel-Lindau tumor suppressor protein. J. Biol. Chem. 275, 25733–25741.
[8] Ohh, M., Park, C.W., Ivan, M., Hoffman, M.A., Kim, T.Y., Huang, L.E., Pavletich, N., Chau, V. and Kaelin, W.G. (2000) Ubiquitination of hypoxia-inducible factor requires direct binding to the beta-domain of the von Hippel-Lindau protein. Nat. Cell Biol. 2, 423–427.
[9] Kamura, T., Sato, S., Iwai, K., Czyzyk-Krzeska, M., Conaway, R.C. and Conaway, J.W. (2000) Activation of HIF1alpha ubiquitination by a reconstituted von Hippel-Lindau (VHL) tumor suppressor complex. Proc. Natl. Acad. Sci. USA 97, 10430–10435.
[10] Tanimoto, K., Makino, Y., Pereira, T. and Poellinger, L. (2000) Mechanism of regulation of the hypoxia-inducible factor-1 alpha by the von Hippel-Lindau tumor suppressor protein. EMBO J. 19, 4298–4309.
[11] Harada, H., Hiraoka, M. and Kizaka-Kondoh, S. (2002) Antitumor effect of TAT-oxygen-dependent degradation-caspase-3 fusion protein specifically stabilized and activated in hypoxic tumor cells. Cancer Res. 62, 2013–2018.
[12] Kizaka-Kondoh, S., Inoue, M., Harada, H. and Hiraoka, M. (2003) Tumor hypoxia: a target for selective cancer therapy. Cancer Sci. 94, 1021–1028.
[13] Inoue, M., Mukai, M., Hamanaka, Y., Tatsuta, M., Hiraoka, M. and Kizaka-Kondoh, S. (2004) Targeting hypoxic cancer cells with a protein prodrug is effective in experimental malignant ascites. Int. J. Oncol. 25, 713–720.
[14] Harada, H., Kizaka-Kondoh, S. and Hiraoka, M. (2005) Optical imaging of tumor hypoxia and evaluation of efficacy of a hypoxia-targeting drug in living animals. Mol. Imaging 4, 182–193.
[15] Fernandes-Alnemri, T., Litwack, G. and Alnemri, E.S. (1994) CPP32, a novel human apoptotic protein with homology toaenorhabditis elegans cell death protein Ced-3 and mammalian interleukin-1 beta-converting enzyme. J. Biol. Chem. 269, 30761–30764.
[16] Iliopoulos, O., Kibel, A., Gray, S. and Kaelin Jr., W.G. (1995) Tumour suppression by the human von Hippel-Lindau gene product. Nat. Med. 1, 822–826.
[17] Johnson, C.R. and Jarvis, W.D. (2004) Caspase-9 regulation: an update. Apoptosis 9, 423–427.
[18] Nagarajah, N.S., Vigneswaran, N. and Zacharias, W. (2004) Hypoxia-mediated apoptosis in oral carcinoma cells occurs via two independent pathways. Mol. Cancer 3, 38.
[19] Mirnezami, A.H., Campbell, S.J., Darley, M., Primrose, J.N., Johnson, P.W. and Blaydes, J.P. (2003) Hdm2 recruits a hypoxia-sensitive corepressor to negatively regulate p53-dependent transcription. Curr. Biol. 13, 1234–1239.
[20] Zhu, Y., Mao, X.O., Sun, Y., Xia, Z. and Greenberg, D.A. (2002) p38 Mitogen-activated protein kinase mediates hypoxic regulation of Mdm2 and p53 in neurons. J. Biol. Chem. 277, 22909–22914.
[21] Alarcon, R., Koumenis, C., Geyer, R.K., Maki, C.G. and Giaccia, A.J. (1999) Hypoxia induces p53 accumulation through MDM2 down-regulation and inhibition of E6-mediated degradation. Cancer Res. 59, 6046–6051.
[22] Graeber, T.G., Peterson, J.F., Tsai, M., Monica, K., Fornace Jr., A.J. and Giaccia, A.J. (1994) Hypoxia induces accumulation of p53 protein, but activation of a G1-phase checkpoint by low-oxygen conditions is independent of p53 status. Mol. Cell. Biol. 14, 6264–6277.
[23] Soengas, M.S., Alarcon, R.M., Yoshida, H., Giaccia, A.J., Hakem, R., Mak, T.W. and Lowe, S.W. (1999) Apaf-1 and caspase-9 in p53-dependent apoptosis and tumor inhibition. Science 284, 156–159.
[24] Rothmann, T., Hengstermann, A., Whitaker, N.J., Scheffner, M. and zur Hausen, H. (1998) Replication of ONYX-015, a potential anticancer adenovirus, is independent of p53 status in tumor cells. J. Virol. 72, 9470–9478.
[25] Bouvet, M., Bold, R.J., Lee, J., Evans, D.B., Abbruzzese, J.L., Chiao, P.J., McConkey, D.J., Chandra, J., Chada, S., Fang, B. and Roth, J.A. (1998) Adenovirus-mediated wild-type p53 tumor suppressor gene therapy induces apoptosis and suppresses growth of human pancreatic cancer. Ann. Surg. Oncol. 5, 681–688.

Acta Oncologica, 2006; 45: 317–324

Taylor & Francis
Taylor & Francis Group

ORIGINAL ARTICLE

Suppression of VEGF transcription in renal cell carcinoma cells by pyrrole-imidazole hairpin polyamides targeting the hypoxia responsive element

YUKIO KAGEYAMA[1], HIROSHI SUGIYAMA[2,3], HIROHITO AYAME[2], AKI IWAI[1], YASUHISA FUJII[1], L. ERIC HUANG[4], SHINAE KIZAKA-KONDOH[5], MASAHIRO HIRAOKA[5] & KAZUNORI KIHARA[1]

[1]*Department of Urology, Graduate School of Tokyo Medical and Dental University, 1-5-45 Yushima, Bunkyo-ku, Tokyo, 113-8519, Japan,* [2]*Institute of Biomaterials and Bioengineering, Tokyo Medical and Dental University, 2-3-10 Surugadai, Kanda, Chiyoda-ku, Tokyo 101-0062, Japan,* [3]*Department of Chemistry, Graduate School of Science, Kyoto University, Kitashirakawa Oiwakecho, Sakyo-ku, Kyoto, 606-8502, Japan,* [4]*Laboratory of Human Carcinogenesis, NCI, National Institute of Health, Bethesda, MD, USA and* [5]*Department of Therapeutic Radiology and Oncology, Graduate School of Medicine, Kyoto University, 54 Kawahara-cho, Shogoin, Kyoto, 606-8507, Japan*

Abstract

Hypoxia inducible factor (HIF), a master regulator of critical genes for cell survival under hypoxic conditions, is known to be related to tumorigenesis and progression of renal cell carcinoma. *N*-methylpyrrole (Py)-*N*-methylimidazole (Im) hairpin polyamides are synthetic organic compounds that recognize and bind to the minor grooves of specific DNA sequences. We synthesized three Py-Im hairpin polyamides targeting the flanking sequences of hypoxia responsive element (HRE; a binding site of HIF) in the promoter region of the vascular endothelial growth factor (VEGF) gene. The effects of the polyamides on HIF-induced transcription were evaluated by a luciferase assay using a reporter plasmid containing a VEGF promoter. Real time reverse-transcriptase polymerase chain reaction and enzyme-linked immunosorbent assay were performed to examine the effects of the polyamides on the transcription and secretion of VEGF in A498 renal cell carcinoma cells, which have a frame-shift mutation in the von Hippel-Lindau gene. A combination of three Py-Im hairpin polyamides suppressed HIF-induced transcription in reporter assays using 293 cells and successfully suppressed transcription and translation of the VEGF gene in A498 cells. Inhibition of the HIF-HRE interaction was confirmed by an electrophoresis mobility shift assay. An approach using Py-Im hairpin polyamides may be a new strategy for the treatment of renal cell carcinoma.

Hypoxia inducible factor (HIF) is a key regulator of molecules that are critical to cell survival under hypoxic conditions [1]. In low-oxygen conditions, HIFs (HIF-1 or HIF-2 bind to the hypoxia responsive element (HRE), and trigger the transcription of target genes such as vascular endothelial growth factor (VEGF) or erythropoietin. Under normal oxygen tension, the von Hippel-Lindau (VHL) protein binds to the alpha subunits of the HIFs (HIF-1α or HIF-2α) and facilitates their rapid degradation.

Renal cell carcinoma is characterized by extensive neovascularization. Recently, frequent mutations of the VHL gene have been demonstrated in familial and sporadic renal cell carcinoma with clear cell phenotypes. Stabilization of HIFs due to an impaired VHL-HIF interaction has been shown to be an underlying mechanism of hypervascularity in renal cell carcinoma [2]. Thus, suppression of transcriptional activity of these HIFs may lead to decreases in de novo vascular formation and provide a new treatment modality for renal cell carcinoma that is resistant to radiation or chemotherapy.

N-methylpyrrole (Py)-*N*-methylimidazole (Im) hairpin polyamides have been shown to bind to the minor groove of specific DNA sequences with affinity and specificity similar to those of

Correspondence: Yukio Kageyama, Department of Urology, Graduate School of Tokyo Medical and Dental University, 1-5-45 Yushima, Bunkyo-ku, 113-8519 Tokyo, Japan. E-mail: kageyys.uro@tmd.ac.jp

(Received 15 September 2005; accepted 21 November 2005)

ISSN 0284-186X print/ISSN 1651-226X online
DOI: 10.1080/02841860500486648

transcriptional factors [3]. Successful suppression of transcription by Py-Im polyamides has been demonstrated for several genes [4]. In the current study, we synthesized three Py-Im hairpin polyamides against sequences flanking the HRE of the human VEGF gene. A combination of three Py-Im hairpin polyamides suppressed HIF-induced transcription in reporter assays and successfully suppressed transcription and translation of the VEGF gene in A498 cells.

Materials and methods

Determination of target sequences

On the basis of the rules of sequence-recognition by Py-Im polyamides [4–6], we designed three Py-Im hairpin polyamides targeting 4–5-base-pair sequences flanking the HRE of the human VEGF gene (Figure 1). Target sequences were set between A/T or T/A pairs according to the reported sequences that successfully suppressed other transcriptional factors [4]. For A/T or T/A, we used a β-alanine pair that degenerately recognizes these base pairs and increases the affinity of the polyamides to the target sequences by correcting intramolecular distortion [7].

Preparation of pyrrole-imidazole hairpin polyamides

N-methylpyrrole (Py)-*N*-methylimidazole (Im) polyamides were synthesized by using a previously described Fmoc solid-phase method [8]. Polyamides were purified by high performance liquid chromatography (HPLC) with a Jasco PU-980 HPLC pump, a UV-975 HPLC UV/VIS detector, and a Chemcobond 5-ODS-H column (4.6 mm × 150 mm). HPLC was performed using 0.1% acetic acid and a linear gradient (20–30% for polyamide no. 1, 10–50% for polyamide no. 2, and 20–30% for polyamide no. 3) of acetonitrile at a flow rate of 1.0 ml/min with detection at 254 nm. Polyamides were eluted at 30.0 min. Structures of the synthesized polyamides were verified by electron spray ionization mass spectra (ESIMS) recorded on a PE Sciex API 165 mass spectrometer. Molecular weights of polyamides measured by ESIMS are listed in Table I. Synthesized polyamides were lyophilized and stored at −20°C, and dissolved in dimethylsulfoxide for the experiments.

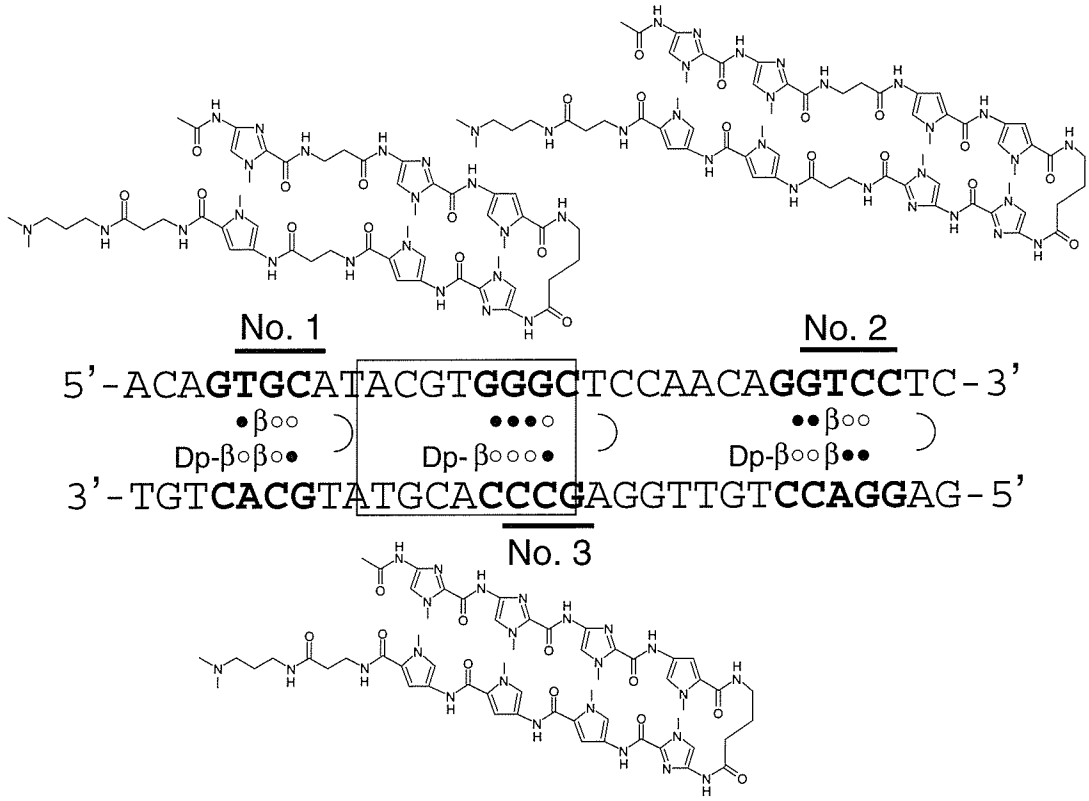

Figure 1. Target sequences and chemical structures of the *N*-methylpyrrole-*N*-methylimidazole hairpin polyamides. Consensus binding site for HIF is indicated by an open box. Open and closed circles represent imidazole and pyrrole rings, respectively. Dp and b denote dimethylaminopropylamine and b-alanine residues, respectively.

Table I. Molecular weights of polyamides measured by ESIMS.

Polyamide	Composition formula	Molecular weight	
		Calculated	Observed
No. 1	$C_{53}H_{71}N_{21}O_{11}$ [M^++H]	1177.56	1178.27
No. 2	$C_{64}H_{82}N_{26}O_{13}$ [M^++H]	1422.66	1423.50
No. 3	$C_{58}H_{72}N_{24}O_{11}$ [M^++H]	1280.58	1281.35

ESIMS, electron spray ionization mass spectra.

Cells and culture conditions

A498 is an established cell line of undifferentiated renal cell carcinoma (American Type Culture Collection, Manassas, VA, USA) that lacks normal expression of the von Hippel-Lindau gene because of a frame-shift mutation at codon 213 [9]. High-level expressions of HIF-1α and HIF-2α in A498 have been demonstrated [10]. 293 is an immortalized human fetal kidney epithelial cell line with very low levels of HIF-1α and HIF-2α under normoxic conditions [10]. Cells were cultured in Dulbecco's modified Eagle's medium (DMEM; Sigma Aldrich, St. Louis, MO, USA) containing 10% fetal bovine serum in a humid chamber with 5% CO_2 at 37°C.

Plasmids

The following plasmids were used to evaluate the effects of the hairpin polyamides on HIF-1α-induced transcription: p(HA)HIF-1α (401Δ603), HA-tagged full-length human HIF-1α with internal deletion of oxygen-dependent degradation domain [11–13]; pTRE-EPAS, full-length human HIF-2α [10]; pARNT, full-length human ARNT [11–13]; pGL3VEGF, pGL3 promoter (Promega, Madison, WI, USA) containing the 385-bp VEGF promoter sequence (−1175 to −790) [14]; pCMVβ (BD biosciences, Palo Alto, CA, USA), a full-length human β-galactosidase cDNA.

Reporter assay

Two hundred and ninety three cells were seeded in 12-well plates (15×10^4 cells per well) and cultured in a humid chamber (5% CO_2). Twenty-four hours later, 0.25 μg of pGL3VEGF, 0.1 μg of p(HA)HIF1α(401Δ 603) or pTRE-EPAS, and 0.1 μg of pARNT were transiently transfected using the FuGene transfection reagent (Roche Applied Science, Penzberg, Germany) according to the manufacturer's protocol. pCMVβ (0.1 μg) was also transfected as a reference plasmid. Two hours later, synthesized polyamides were added to the culture. Doses and combinations of the polyamides are shown in the figures. After incubation for another 24 h, cells were lyzed with M-PER reagent (Pierce, Rockford, IL, USA). Luciferase activity was determined with the Bright-Glo™ Luciferase assay system (Promega, Madison, WI, USA). The luminescence signal was evaluated by using a Gene Light 55 luminometer (Microtec, Tokyo, Japan). The activity of β-galactosidase was measured by using a mammalian β-galactosidase assay kit (Pierce, Rockford, IL, USA) and an MT Max microplate reader (Wako, Tokyo, Japan). Assays were carried out in triplicate and repeated at least twice. The results were expressed as a ratio of luciferase activity to β-galactosidase activity.

Real-time reverse transcriptase-polymerase chain reaction

A498 cells were seeded in 6-well plates (30×10^4/well). The medium was replaced 24 h later and a polyamide mixture (5 μM in total) was added to the culture. Total RNA was extracted from the cells after 24, 48, and 72 h using ISOGEN (Nippon Gene, Tokyo, Japan), an RNA-isolating reagent. cDNA was synthesized from 5 μg of the total RNA samples using the SuperScript™ First-Strand Synthesis System for reverse transcriptase-polymerase chain reaction (RT-PCR; Invitrogen, Carlsbad, CA, USA). Five microliters of 500-fold-diluted cDNA samples were subjected to real time PCR by using a Light Cycler™ real time PCR instrument (Roche Applied Science, Penzberg, Germany). Light Cycler™ primer sets for human VEGF or human GAPDH (Serach LC, Heidelberg, Germany) were used together with LightCycler FastStart DNA Master SYBR Green I (Roche Applied Science, Penzberg, Germany). Results were expressed as a ratio of VEGF mRNA to GAPDH mRNA. Experiments were carried out in triplicate and repeated at least twice.

Enzyme-linked immunosorbent assay

A498 cells were plated on 24-well plates (5×10^4/well). The medium was replaced 24 h later and a polyamide mixture (5 μM in total) was added to the culture. Conditioned media were collected after 24, 48 and 72 h. The concentration of VEGF in the conditioned media was measured by using a Cytokine Enzyme-Linked Immunosorbent Assay (ELISA) Human VEGF Kit (American Research Products, Belmont, MA, USA). Assays were carried out in triplicate and repeated at least twice. Results were expressed as a ratio of VEGF concentration to total protein concentration, which was determined by using the BCA™ Protein Assay Kit (Pierce, Rockford, IL, USA).

Cell viability assay

A498 or 293 cells were seeded in 24-well plates. The medium was replaced 24 h later and polyamides at designated concentrations were added to the culture. After 24 h of incubation, the viability of the cells was assessed by using a CellTiter 96 AQueous One Solution Cell Proliferation Assay reagent (Promega, Madison, WI, USA). For A498, viability at 48 and 72 h was also measured. All assays were carried out in triplicate and repeated at least twice.

Electrophoresis mobility shift assay

Nuclear extract (100 µl) was prepared from 1×10^6 A498 cells using the NE-PER Nuclear and Cytoplasmic Extraction Reagent (Pierce, Rockford, IL, USA) according to the manufacturer's instructions. The binding reaction was carried out by using a Light-Shift Chemiluminescent Electrophoresis Mobility Shift Assay (EMSA) Kit (Pierce, Rockford, IL, USA). Twenty femtomoles of a biotin-labeled double-stranded oligonucleotide (5′-GTGCATACGTGGGCTCCAACAGGTCC-3′) corresponding to the sequence harboring the HRE of the human VEGF gene was mixed with 10 nmol of the polyamide mixture (no. 1, 2 or 3) or a polyamide targeting the human telomere sequence (TTAGGG) [15] in 20 µl of 1x binding buffer containing 2.5% glycerol, 5 mM $MgCl_2$, 50 ng/µl poly(dIdC), and 0.05% NP40. The reaction mixture was incubated for 20 min at room temperature, mixed with 2 µl of the A498 nuclear extract, and then incubated for another 20 min at room temperature. The nuclear extract was substituted with an equal volume of H_2O in a negative control. In a positive control, polyamide samples were replaced by an equal volume of H_2O. The reaction products were mixed with 5x loading buffer, electrophoresed in a 6% polyacrylamide gel (Invitrogen, Carlsbad, CA, USA) in 0.5x Tris-borate-EDTA (TBE), and transferred to a nylon membrane (Pierce, Rockford, IL, USA). Biotin-labeled DNA was detected by using a Chemiluminescent Nucleic Acid Detection Module (Pierce, Rockford, IL, USA) according to the manufacturer's instructions and analyzed by using an LAS-1000 imaging system (Fujifilm, Tokyo, Japan).

Results

Dose-dependent suppression of HIF-1α-induced transcription by polyamide mixture

We evaluated the effects of the synthesized polyamides on HIF-1α -induced transcription by using a reporter assay. A luciferase-expressing vector with the promoter region of the human VEGF gene was used as a reporter plasmid. Because HIF-1α is fairly unstable under normal oxygen tension, we used a stable HIF-1α construct that is transcriptionally active. Because HIF-1α makes a heterodimer with ARNT (also known as HIF-1α) for binding to the HRE, a plasmid clone of the human ARNT gene was transfected along with the HIF-1α. A plasmid containing the human β-galactosidase gene was also transfected and used as a reference standard. As shown in Figure 2, a combination of three hairpin polyamides suppressed transcription induced by HIF-1α in a dose-dependent manner to 56% of the control (vehicle only). The viability of the cells was not affected.

Suppression of HIF-1α-induced transcription by a combination of the three hairpin polyamides

The effects of each polyamide alone and various combinations of the three polyamides were evaluated by using a reporter assay. As shown in Figure 3, of the three polyamides, no.2 was the most potent suppressor of HIF-induced transcription at a concentration of 5 µM. A combination of all three polyamides, however, resulted in satisfactory

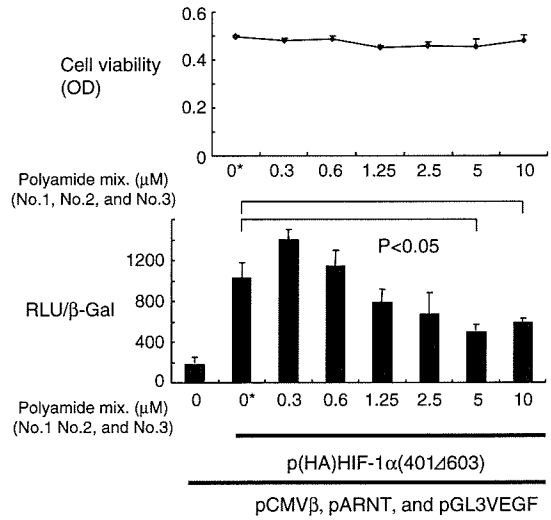

Figure 2. Dose-dependent inhibition of HIF-1α-induced transcription in 293 cells. Cells were transfected with plasmids coding hypoxia-stable HIF-1α, ARNT, and β-galactosidase, along with a reporter plasmid (pGL3VEGF), and then treated with the mixture of three pyrrole-imidazole hairpin polyamides for 24 h. Transcriptional activity was measured and expressed as a ratio of luciferase to β-galactosidase activity. Statistically significant suppression of transcription was noted at a concentration of 5 µM or greater. Cell viability was not affected by the polyamides. RLU and β-Gal denote relative luciferase units and β-galactosidase activity, respectively. OD: optical density. *: Vehicle (dimethylsulfoxide) only.

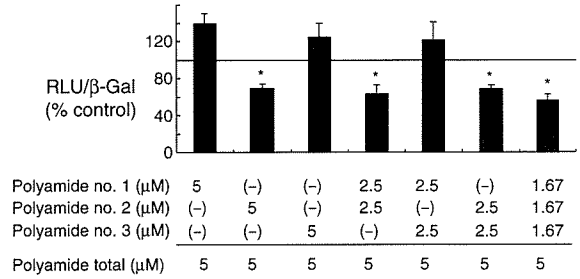

Figure 3. Effects of combinations of the three polyamides on HIF-1α -induced transcription in 293 cells. Cells were transfected with plasmids coding for hypoxia-stable HIF-1α(p(HA) HIF-1α(401Δ603)), ARNT (pARNT), and β-galactosidase (pCMVβ), along with a reporter plasmid (pGL3VEGF), and then incubated with a particular combination of the pyrrole-imidazole polyamides for 24 h. Transcriptional activity was expressed as a ratio of luciferase to β-galactosidase activity. A statistically significant reduction in transcription was achieved by applying all three Py-Im hairpin polyamides. A similar suppression was observed when polyamide no. 3 was applied alone or together with either polyamide no. 1 or no. 2. Cell viability was not affected by the treatment. RLU and β-Gal represent relative luciferase units and β-galactosidase activity, respectively. *:P <0.05 compared with controls.

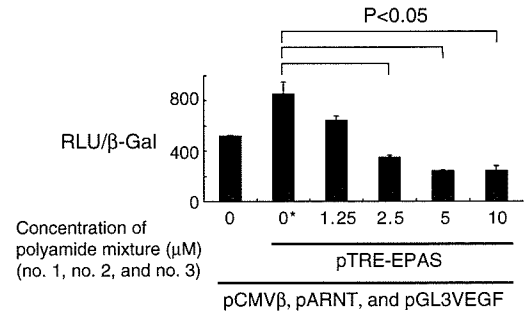

Figure 4. Dose-dependent inhibition of HIF-2α-induced transcription in 293 cells. Cells were transfected with plasmids coding full-length HIF-2α (pTRE-EPAS), ARNT(pARNT), and β-galactosidase (pCMVβ), along with a reporter plasmid (pGL3VEGF), and then treated with a mixture of the three pyrrole-imidazole hairpin polyamides for 24 h. Transcriptional activity was measured and expressed as a ratio of luciferase to β-galactosidase activity. Statistically significant suppression of transcription was noted at a concentration of 2.5 μM or greater. RLU and β-Gal denote relative luciferase units and β-galactosidase activity, respectively. *: Vehicle (dimethylsulfoxide) only.

suppression at lower concentrations of each polyamide compared with the monotreatment.

Suppression of HIF-2α-induced transcription by the polyamide mixture

We also examined the effects of the polyamide mixture on HIF-2α-induced transcription by using a reporter assay. A luciferase-expressing vector with the promoter region of the human VEGF gene was used as a reporter plasmid. As in the experiments using HIF-1α, a plasmid clone of the human ARNT gene was co-transfected with a full-length clone of the human HIF-2α gene. A plasmid containing the human β-galactosidase gene was also transfected and used as a reference standard. As shown in Figure 4, a combination of the three hairpin polyamides suppressed transcription induced by HIF-2α in a dose-dependent manner to 28% of the control (vehicle only).

Suppression of transcription and secretion of VEGF in renal cell carcinoma cells by the polyamide mixture

We examined the effects of the mixture of all three polyamides on VEGF transcription in renal cell carcinoma cells by using real-time RT-PCR. GAPDH mRNA was used as an internal standard. We used A498, a cell line derived from human renal cell carcinoma, with a frame-shift mutation in the VEGF gene. As shown in Figure 5, the polyamide mixture at a concentration of 5 μM inhibited VEGF transcription in A498 cells in a time-dependent manner. An approximately 50% reduction in VEGF transcription relative to the control (vehicle only) was observed when cells were exposed to the polyamide mixture for 72 h. Inhibition of VEGF at the protein level was examined by ELISA using conditioned media. The results were consistent with those of real-time RT-PCR. Secretion of VEGF was suppressed by the polyamide mixture in a time-dependent manner. The amount of VEGF in the conditioned media was reduced to approximately 50% of the control (vehicle only) by exposing A498 cells to the polyamide mixture for 72 h. The viability of A498 cells was not affected by incubation with the Py-Im polyamides.

Specific inhibition of HIF-HRE binding by the polyamide mixture

EMSA was carried out to confirm the inhibitory effects of the polyamide mixture on HIF-HRE binding (Figure 6). Addition of the A498 nuclear extract to the reaction mixture caused an apparent mobility shift of the biotin-labeled DNA, which was suppressed by the polyamide mixture recognizing the human HRE. The mobility shift was not affected by a polyamide recognizing the human telomere sequence, which was used as a control.

Statistics

Each assay was carried out in triplicate and repeated at least twice. Statistical significance was analyzed by using Student's t-test.

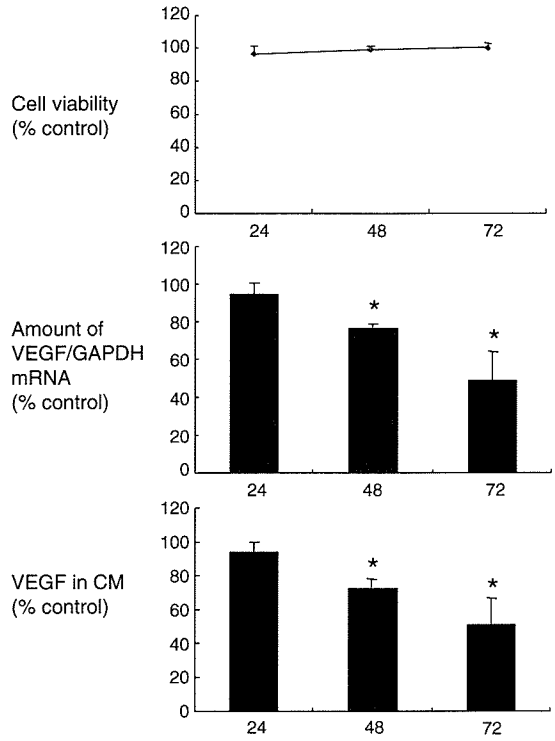

Figure 5. Suppressive effects of the mixture of three Py-Im hairpin polyamides on VEGF transcription and secretion in A498, a renal cell carcinoma cell line. Cells were treated with the mixture of three pyrrole-imidazole polyamides (5 mM in total) for 24–72 h. Transcription of the VEGF gene was evaluated by real time RT-PCR. The results were expressed as a ratio of VEGF mRNA to GAPDH mRNA. An approximately 50% reduction in transcription was observed after 72 h treatment. Consistently, VEGF secreted in conditioned medium (CM) decreased by approximately 50% compared with the control. *: $P < 0.05$ compared with controls.

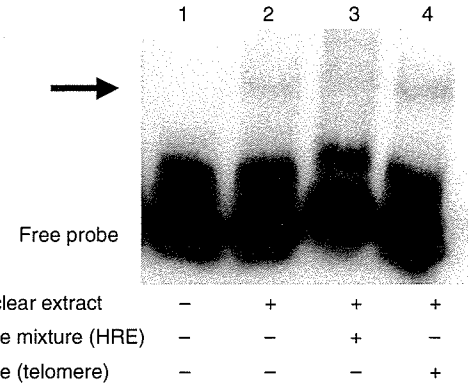

Figure 6. Inhibitory effects of pyrrole-imidazole hairpin polyamides on the HIF-HRE interaction were evaluated by using an electrophoresis mobility shift assay. Nuclear extract of A498 human renal cell cancer cells caused a mobility shift (arrow) of a biotin-labeled double-stranded oligonucleotide corresponding to human HRE (lanes 1 and 2). The polyamide mixture against the HRE suppressed the mobility shift (lane 3), which was not affected by a polyamide recognizing the human telomere sequence (lane 4).

Discussion

VEGF transcription in renal cell carcinoma cells was effectively suppressed by the Py-Im hairpin polyamides in the current study. Inhibition of the HIF-HRE interaction was confirmed by EMSA to be the underlying mechanism of this suppression. The hairpin polyamide strategy was pioneered by Dervan and colleagues [3]. Py and Im covalently link side-by-side in an anti-parallel arrangement that has been shown to recognize and bind to specific DNA sequences [4–6]. Im-Py recognizes G:C, whereas Py-Im recognizes C:G. The Py-Py pair recognizes A:T or T:A base pairs. The hydroxypyrrole and Py pair (Hp–Py) distinguishes T:A from A:T and vice versa. Placing a β-alanine pair, which degenerately binds to T:A or A:T, increases the affinity and specificity for sequences by relaxing the rigid curvature of polyamides [7]. Following these rules, regulation of gene expression by Py-Im hairpin polyamides has been successfully demonstrated for a variety of transcriptional factors, including Ets-1, TATA box (TBP) binding protein and lymphoid enhancer factor (LEF) 1 [4]. Our data suggest that HIF-induced transcription can also be controlled effectively by competitive binding of multiple Py-Im hairpin polyamides.

In the current study, we prepared three polyamides recognizing 4–5 base pairs flanking the HRE of the VEGF gene, and administered them together to obtain maximum specificity. Because of technical constraints, it is difficult to synthesize long polyamide chains. Moreover, the longer the target sequence is, the greater the intramolecular distortion becomes. Thus, Py-Im hairpin polyamides against 4–5-base-pair sequences have been used in most studies. Recently, a hairpin polyamide that recognizes TACG within the HRE has been reported to inhibit VEGF transcription [16]. Treatment with a combination of multiple polyamides is another option, and may increase the efficacy of treatment with Py-Im hairpin polyamides.

Py-Im hairpin polyamides have advantages as modulators of gene expression [4]. First, their low molecular weight allows them to permeate through cell membranes: they simply pass through cell membranes and reach their target sites without special aids or vehicles such as expression vectors or liposomes. Designing hairpin polyamides is not

difficult, and automated solid-phase synthesis is possible. Moreover, they have flexible sites for covalent attachment to other molecules. Hairpin polyamides linked with an alkylating agent may broaden the targets of transcriptional regulation of coding sequences [17]. In fact, we have successfully inhibited gene transcription of the green fluorescent protein and luciferase by alkylating hairpin polyamides [18].

Inhibiting the HIF transcription pathway is a fascinating strategy for cancer control, especially in the case of renal cell carcinomas. HIF controls genes related to the progression of cancers. Genes for platelet-derived growth factor (PDGF), VEGF, epidermal growth factor (EGF), and transforming growth factor-1α (TGF-1α are among those regulated by HIF-1 (a dimer of HIF-1α and ARNT). Therapeutic approaches using each of these molecules are being trialled clinically [19]. Avastin™ (anti-VEGF antibody), SU11248 (a small molecule targeting the tyrosine kinase domain of the VEGF receptor), and Tarceva™ or Iressa™ (molecules targeting the tyrosine kinase domain of the EGF receptor) are currently being investigated as potential agents against advanced renal cell carcinoma. Recently, we have shown that glucocorticoids can down-regulate VEGF in renal cell carcinoma cells [20]. Suppressing the binding of HIF-1 to the HRE may be a useful strategy for inhibition of these molecules. In addition, we and several other groups have demonstrated that HIF-2α, another α subunit of HIF, is more critical than HIF-1α in renal cell cancer [10,21]. As HIF-2 (a dimer of HIF-2α and ARNT) shares an HRE with HIF-1, targeting the HIF-HRE interaction may be more useful in the management of renal cell carcinoma than using the molecular therapeutic drugs described earlier. In the current study, the polyamide mixture successfully suppressed transcription induced not only by HIF-1α but also by HIF-2α. Our findings may facilitate the realization of the "transcription therapy" concept proposed by Dervan [5] for cancer treatment.

Conclusions

VEGF transcription was successfully suppressed by a combination of three Py-Im hairpin polyamides targeting the HRE. The use of Py-Im hairpin polyamides may be a new strategy for the treatment of renal cell carcinoma.

Acknowledgements

We thank Dr. Minori Koshiji and Ms. Kaoru Ito for their technical support. This work was supported by a Grant-in-Aid (14370505, 17591666, 17591667) for Scientific Research from the Ministry of Education, Science and Culture, Japan.

References

[1] Huang LE, Bunn HF. Hypoxia inducible factor and its biomedical relevance. J Biol Chem 2003;278:19575–8.
[2] Kaelin WG. The von Hippel-Lindau tumor suppressor gene and kidney cancer. Clin Cancer Res 2004;10:6290–5s.
[3] White S, Szewczyk JW, Turner JM, Baird EE, Dervan PB. Recognition of the four Watson-Crick base pairs in the DNA minor groove by synthetic ligands. Nature 1998;391:468–71.
[4] Murty MSRC, Sugiyama H. Biology of N-methylpyrrole-N-methylimidazole hairpin polyamide. Biol Pharm Bull 2004; 27:468–74.
[5] Dervan PB. Molecular recognition of DNA by small molecules. Bioorg Med Chem 2001;9:2215–35.
[6] Kielkopf CL, White S, Szewczyk JW, et al. A structural basis for recognition of A.T and T.A base pairs in the minor groove of B-DNA. Science 1998;282:111–5.
[7] Wang CC, Ellervik U, Dervan PB. Expanding the recognition of the minor groove of DNA by incorporation of beta-alanine in hairpin polyamides. Bioorg Med Chem 2001;9: 653–7.
[8] Ayame H, Saito T, Bando T, Fukuda N, Sugiyama H. Fmoc solid-phase synthesis and its application to pyrrole-imidazole polyamides. Nucleic Acids Res 2003;3:67–8s.
[9] Gnarra JR, Tory K, Weng Y, Schmidt L, Wei MH, Li H, et al. Mutations of the VHL tumor suppressor gene in renal carcinoma. Nature Genet 1994;7:85–90.
[10] Xia G, Kageyama Y, Hayashi T, Kawakami S, Yoshida M, Kihara K. Regulation of vascular endothelial growth factor transcription by endothelial PAS domain protein 1 (EPSA1) and possible involvement of EPAS1 in the angiogenesis of renal cell carcinoma. Cancer 2001;91:1429–36.
[11] Huang LE, Gu J, Schau M, Bunn HF. Regulation of hypoxia inducible factor 1α is mediated by an O2-dependent degradation domain via an ubiquitin-proteasome pathway. Proc Natl Acad Sci USA 1998;95:7978–92.
[12] Kageyama Y, Koshiji M, To KKW, Tian YM, Ratcliffe PJ, Huang LE. Leu-574 of human HIF-1a is a molecular determinant of prolyl hydroxylation. FASEB J 2004;18: 1028–30.
[13] Koshiji M, Kageyama Y, Pete EA, Horikawa I, Barret JC, Hunag LE. HIF-1α induces cell cycle arrest functionally counteracting Myc. EMBO J 2004;23:1949–56.
[14] Shibata T, Akiyama N, Noda M, Sasai K, Hiraoka M. Enhancement of gene expression under hypoxic conditions using fragments of the human vascular endothelial growth factor and the erythropoietin genes. Int J Radiat Oncol Biol Phys 1998;42:913–26.
[15] Takahashi R, Bando T, Sugiyama H. Specific alkylation of human telomere repeats by hairpin pyrrole-imidazole polyamide. Bioorg Med Chem 2003;11:2503–9.
[16] Olenyuk BZ, Zhang GJ, Klco JM, Nickols NG, Kaelin WG Jr, Dervan PB. Inhibition of vascular endothelial growth factor with a sequence-specific hypoxia response element antagonist. Proc Natl Acad Sci USA 2004;101: 16768–73.
[17] Oyoshi T, Kawakami W, Narita A, Bando T, Sugiyama H. Inhibition of transcription at a coding sequence by alkylating polyamide. J Am Chem Soc 2003;125:4752–4.

[18] Shinohara K, Narita A, Oyoshi T, Bando T, Teraoka H, Sugiyama H. Sequence-specific gene silencing in mammalian cells by alkylating pyrrole-imidazole polyamides. J Am Chem Soc 2004;126:5113–8.

[19] Linehan WM, Vasselli J, Srinivasan R, Walther MM, Merino M, Choyke P, et al. Genetic basis of cancer of the kidney: disease-specific approaches to therapy. Clin Cancer Res 2004;10:6282–9s.

[20] Iwai A, Fujii Y, Kawakami S, Takazawa R, Kageyama Y, Yoshida MA, et al. Down-regulation of vascular endothelial growth factor in renal cell carcinoma cells by glucocorticoids. Mol Cell Endocrinol 2004;226:11–7.

[21] Seagroves T, Johnson RS. Two HIFs may be better than one. Cancer Cell 2002;1:211–3.

0013-7227/06/$15.00/0
Printed in U.S.A.

Endocrinology 147(2):733–743

doi: 10.1210/en.2005-0679

Thioredoxin-Binding Protein-2-Like Inducible Membrane Protein Is a Novel Vitamin D3 and Peroxisome Proliferator-Activated Receptor (PPAR)γ Ligand Target Protein that Regulates PPARγ Signaling

Shin-ichi Oka, Hiroshi Masutani, Wenrui Liu, Hiroyuki Horita, Dongmei Wang, Shinae Kizaka-Kondoh, and Junji Yodoi

Institute for Virus Research (S.O., H.M., W.L., H.H., D.W., J.Y.), Kyoto University, Kyoto 606-8507, Japan; and Department of Therapeutic Radiology and Oncology (S.K.-K.), Kyoto University Graduate School of Medicine, Kyoto University, Yoshida-konoe-cho, Sakyo, Kyoto 606-8501, Japan

Thioredoxin binding protein-2 (TBP-2), which is identical with vitamin D3 (VD3) up-regulated protein 1 (VDUP1), plays a crucial role in the integration of glucose and lipid metabolism. There are three highly homologous genes of TBP-2/vitamin D3 up-regulated protein 1 in humans, but their functions remain unclear. Here we characterized a TBP-2 homolog, TBP-2-like inducible membrane protein (TLIMP). In contrast to TBP-2, TLIMP displayed no significant binding affinity for thioredoxin. TLIMP exhibited an inner membrane-associated pattern of distribution and also colocalized with transferrin and low-density lipoprotein, indicating endosome- and lysosome-associated functions. VD3 and ligands of peroxisome proliferator-activated receptor (PPAR)-γ, an important regulator of energy metabolism and cell growth inhibition, induced the expression of TLIMP as well as TBP-2. Overexpression of TLIMP suppressed both anchorage-dependent and -independent cell growth and PPARγ ligand-inducible gene activation. These results suggest that TLIMP, a novel VD3- or PPARγ ligand-inducible membrane-associated protein, plays a regulatory role in cell proliferation and PPARγ activation. (*Endocrinology* 147: 733–743, 2006)

IT IS WELL established that vitamin D3 (VD3) acts as a modulator of cell growth, differentiation, maintenance of extracellular calcium levels, bone mineralization, and lipid metabolism. VD3 exerts its actions through nuclear VD3 receptor (VDR)-mediated signal transduction and gene transcription (1). Another well-established nuclear receptor subfamily, peroxisome proliferator-activated receptors (PPARs), comprising PPARα, -δ (β), and -γ, binds fatty acids and play important roles in energy homeostasis. Thiazolidine derivatives, such as troglitazone and pioglitazone, which are selective PPARγ agonists, reduce hyperlipidemia in obese and diabetic animals (2–5). VDR and/or PPARs regulate gene transcription to modulate uptake of calcium, phosphate, lipids, and glucose from plasma (6, 7). In addition, several reports have suggested that VDR and PPARs have a regulatory role in the uptake of plasma proteins (8–11). However, the regulatory role and mechanisms of the membrane-associated function of VDR and PPARs largely remains to be clarified.

First Published Online November 3, 2005

Abbreviations: DTT, Dithiothreitol; EF, elongation factor; EGFP, enhanced green fluorescent protein; FABP4, fatty acid-binding protein 4; FCS, fetal calf serum; FITC, fluorescein isothiocyanate; GST, glutathione-S-transferase; LDL, low-density lipoprotein; LPL, lipoprotein lipase; PMA, phorbol 12-myristate 13-acetate; PPAR, peroxisome proliferator-activated receptor; RA, retinoic acid; TBP-2, thioredoxin binding protein-2; TLIMP, TBP-2-like inducible membrane protein; TRX, thioredoxin; VD3, vitamin D3; VDUP1, vitamin D3 up-regulated protein 1.

Endocrinology **is published monthly by The Endocrine Society (http://www.endo-society.org), the foremost professional society serving the endocrine community.**

In the course of our study of thioredoxin (TRX), an important redox regulator (12, 13), we identified TRX-binding protein (TBP)-2 (14), which is identical with VD3 up-regulated protein 1 (VDUP1), a VD3-inducible gene in HL-60 cells (15). Several reports show that loss of TBP-2 expression is associated with cell growth or transformation. TBP-2 is down-regulated in human T cell leukemia virus I-transformed cells and human cancer tissues (16–19), whereas overexpression of TBP-2 induces cell growth suppression (18–20). Interestingly, HcB-19 mice, which have a nonsense mutation in the TBP-2 gene, exhibit hyperlipidemia characterized by elevated plasma triglyceride and/or cholesterol levels (21). The analyses of the HcB-19 mice (22) or TBP-2 knockout mice (23) revealed that TBP-2 plays a critical role in the integrated regulation of glucose and lipid metabolism in fasting. The molecular mechanisms underlying transformation and hyperlipidemia caused by loss of TBP-2 function remain to be elucidated, as does the mechanism behind the physiological function of TBP-2.

In this paper, we report that there are three homologous TBP-2/VDUP1 genes in humans. The TBP-2 homologs constitute a family and are preserved in *Schizosaccharomyces pombe*, *Saccharomyces cerevisiae*, *Drosophila melanogaster*, and *Caenorhabditis elegans* but not *Escherichia coli*, indicating that the genes have evolutionarily conserved roles in the eukaryotic system. However, the functions of these family members have not been clarified. Characterization of members of the human TBP-2 family will provide new insights into the biological roles of these genes. We have cloned a human TBP-2 homolog, TBP-2-like inducible membrane protein (TLIMP),

and show that TLIMP and TBP-2 are VD3/PPARγ ligand-inducible genes. To investigate the biological role of the TBP-2 gene family and understand the molecular mechanism of the VD3/PPAR-mediated cellular function, we characterized TLIMP and investigated the role of TLIMP in cellular growth regulation and PPARγ ligand-induced gene activation.

Materials and Methods

Reagents and materials

Phorbol 12-myristate 13-acetate (PMA), clofibrate, and prostaglandin J2 were purchased from Sigma (St. Louis, MO). Blasticidin was purchased from Kaken Pharmaceutical Co., Ltd. (Tokyo, Japan). Complete protease inhibitor cocktail was purchased from Roche Applied Science (Mannheim, Germany). Total RNAs from human cultured preadipocytes and adipocytes were purchased from Zen-Bio, Inc. (Research Triangle Park, NC). The human adipocytes were differentiated from preadipocytes by culturing with insulin and dexamethasone for 14 d. Troglitazone and pioglitazone were kindly provided by Sankyo Pharmaceutical Co. (Tokyo, Japan) and Takeda Pharmaceutical Co., Ltd. (Tokyo, Japan), respectively. L165,041 was purchased from Calbiochem (La Jolla, CA). Alexa-633-labeled transferrin, BODIPY FL-labeled low-density lipoprotein, fluorescein isothiocyanate (FITC)-conjugated antimouse IgG, Alexa 568-conjugated antimouse IgG, and LysoTracker Blue were purchased from Molecular Probes (Eugene, OR). Human 12-lane multiple tissue and cancer cell line Northern blots were obtained from CLONTECH (Mountain View, CA).

Amino acid sequence alignment

Amino acid sequences of TBP-2 family proteins were aligned using the ClustalW program (EMBL-European Bioinformatics Institute) and the BOXSHADE program (Swiss Institute of Bioinformatics) was used for formatting the results.

Plasmids

The open reading frame of TLIMP was amplified by PCR using the oligonucleotide primers 5′-AATGGATCCATGGTGCTGGGAAAGGTGAA-3′ and 5′-CGAATTCAACGAGAGGGGCAGGAT-3′. The cDNAs were subcloned into pCMV-Tag2B (CLONTECH) and pGEX6P1 (Amersham Biosciences, Piscataway, NJ) to generate pCMV-Flag-TLIMP and pGST-TLIMP, respectively. pEF-BSR, a blasticidin-resistant mammalian expression vector driven by the elongation factor (EF) 1 promoter, was kindly provided by Dr. Ishii (Riken Research Center for Allergy and Immunology, Yokohama, Japan). The cDNA containing a Kozak sequence in the 5′ side of the TLIMP gene lacking a stop codon was obtained by PCR using oligonucleotide primers 5′-GGAATTCGCCACCATGGTGCTGGGAAAGGT-3′ and 5′-CGGGATCCACGAGAGGGGCAGGATGGTCTA-3′. The TLIMP cDNA was ligated into pEF-BSR downstream of the EF promoter, and then a DNA fragment encoding the Flag epitope or enhanced green fluorescent protein (EGFP; pEGFP-N3; CLONTECH) was inserted into the 3′ end of TLIMP to generate pEF-BSR-TLIMP-Flag or pEF-BSR-TLIMP-EGFP, respectively. The N-terminal Flag epitope-tagged TBP-2 cDNA was ligated into pEF-BSR to generate pEF-BSR-Flag-TBP-2. Yeast expression vectors, pGBKT7-TLIMP and pGBKT7-TBP-2, for the expression of TLIMP or TBP-2 fused with the GAL4 DNA-binding domain were constructed by insertion of the open reading frames of TLIMP and TBP-2 into pGBKT7 (CLONTECH). The cDNA of TRX was ligated into pACT2 (CLONTECH) to generate pACT2-TRX, an expression vector for the GAL4 activation domain fused with TRX. Luciferase reporter plasmids containing five GAL4 binding sites in the promoter region (pGAL4-luc), and plasmid expressing PPARγ2 fused to the GAL4 DNA binding domain (pM-PPARγ2) and HA-tag (pcDNA3-HA-PPARγ2) were kindly provided by Dr. Ohshima (24).

Cell culture and transfection

HL-60 cells were cultured in RPMI 1640 medium. HeLa S3, COS7, and 293 cells were cultured in DMEM. CHO cells were cultured in F-12 medium. Heat-inactivated fetal calf serum (FCS) and antibiotics were added to the media. Cells were transfected with Lipofectamine (Invitrogen, Carlsbad, CA), according to the manufacturer's instructions. Stable transfectants were generated by transfection of HeLa S3 cells with either pEF-BSR-TLIMP-Flag or pEF-BSR control plasmid. After 24 h, cells were plated and selected in medium containing 4 μg/ml blasticidin. The expression of TLIMP in the transfectants was confirmed by Western blotting analyses. Reporter assay were performed as described previously (25). NIH3T3 cells were transfected with the TLIMP and GAL4-PPARγ2 expression vectors and luciferase reporter plasmids containing five GAL4 binding sites in the promoter region. Cells were then treated with troglitazone and luciferase reporter assay were performed (24).

Northern blotting analysis

Total RNA from cells was extracted using TRIzol reagent (Invitrogen), according to the manufacturer's instructions. Total RNA (10–20 μg/lane) was fractionated by denaturing agarose gel electrophoresis and transferred to a nylon membrane (Hybond N^+; Amersham Biosciences). The blots were hybridized with a [^{32}P]-labeled probe prepared using the BcaBest labeling kit (Takara, Shiga, Japan) overnight at 68 C.

Semiquantitative RT-PCR

Total RNAs from cells and tissues were extracted using TRIzol reagent (Invitrogen), according to the manufacturer's instructions. Reverse transcription was performed with a SuperScript III first-strand synthesis system kit (Invitrogen). PCRs were carried out using the following oligonucleotide primers: human TLIMP forward primer, 5′-ATGGTGCTGGGAAAGGTGAA-3′, and reverse primer, 5′-TCAACGAGAGGGGCAGGAT-3′; human TBP-2 forward primer, 5′-AAGGTGCTGACTCAGAAG-3′, and reverse primer, 5′-CTCACTGCACATTGTTGTTG-3′; human glyceraldehyde-3-phosphate dehydrogenase forward primer, 5′-ATGGGGAAGGTGAAGGTCGGAGTC-3′, and reverse primer, 5′-CCATGCCAGTGAGCTTCCCGTTC-3′; mouse TLIMP forward primer, 5′-ACAGTTACAGTGCCTGAGAAGACTCGG-3′, and reverse primer, 5′-GTGCCCTCAGGTGTTACGTCAAG-3′; mouse TBP-2 forward primer, 5′-GTGATGGATCTAGTGGATGTC-3′, and reverse primer, 5′-TCACTGCACGTTGTTGTTG-3′; mouse fatty acid-binding protein 4 (FABP4) forward primer, 5′-ACAAAATGTGTGATGCCTTTGTGGGAAC-3′, and reverse primer, 5′-TCCGACTGACTATTGTAGTGTTTGATGCAA-3′; mouse lipoprotein lipase (LPL) forward primer, 5′-GGGGTACCTGCCCACCACTTGTCCCCTGGAG-3′, and reverse primer, 5′-CGGGATCCCGGTGCACCCTTCTGCTTTGCTGC-3′; and mouse β-actin forward primer, 5′-ATGGATGACGATATCGCTGCGCT-3′, and reverse primer, 5′-TAGAAGCACTTGCGGTGCACGAT-3′. Amplification of the products is not saturated with the number of cycles performed.

Western blotting analysis

Cell lysates or immunoprecipitates were fractionated by SDS-PAGE and then transferred to a polyvinylidene difluoride membrane (Amersham Biosciences). Western blot analysis was performed using an enhanced chemiluminescence Western blotting detection system (Amersham Biosciences), according to the manufacturer's instructions.

Subcellular fractionation

Cells (at confluence in a 3.5 cm dish) were lysed with lysis buffer [25 mM Tris-HCl (pH 7.8), 2 mM dithiothreitol (DTT), 10% glycerol, 1% Trition X-100, and 1× complete protease inhibitor cocktail] and the cell lysate was centrifuged at 100,000 × *g* for 10 min. The supernatant, the Triton X-100 soluble fraction (100 μl) was transferred to a new tube, and 25 μl of 5× sample buffer [500 mM Tris-HCl (pH 6.8), 10% sodium dodecyl sulfate, 25% glycerol, 12.5% 2-mercaptoethanol, and 0.25% bromophenol blue] was added. The pellet, the Triton X-100 insoluble fraction, was resuspended with 125 μl of 1× sample buffer (5-fold dilution of 5× sample buffer with lysis buffer) before sonication. The fractionated samples were subjected to Western blotting analyses.

Immunofluorescent staining

Cells were cultured on glass-bottom dishes, fixed with 4% paraformaldehyde in PBS for 5 min at room temperature, and permeabilized for

5 min using 1% Nonidet P-40 in PBS. The permeabilized cells were incubated in PBS containing 1.5% FCS and then with anti-Flag antibody (Sigma) or anti-Myc antibody (Santa Cruz Biotechnology, Santa Cruz, CA), followed by FITC- or Alexa 568-conjugated antimouse IgG. The immunostained cells were examined with a confocal microscope (Leica Microsystems, Mannheim, Germany).

Preparation of recombinant proteins and in vitro binding assay

In vitro-translated proteins were prepared using a TNT-coupled rabbit reticulocyte translation system (Promega, Madison, WI). The [^{35}S]methionine-labeled translated products were analyzed by SDS-PAGE after performance of a glutathione-S-transferase (GST) pull-down assay. GST-TRX was prepared as described previously (14). The precipitates were detected by autoradiography using a Bio-image analyzer BAS2000 (Fuji Film Co. Ltd., Tokyo, Japan) or Coomassie Brilliant Blue staining.

Insulin-reducing assay

COS7 cells were transiently transfected with the GFP-TBP-2 or TLIMP expression vector. After 3 d, the cells (at confluence in a 10 cm dish) were collected and lysed by the freeze and thaw method. The cell lysate (10 mg/ml, 10 μl) was preincubated with 2.5 μl DTT activation buffer [0.1 M Tris-HCl (pH 7.5), 2 mM EDTA, 1 mg/ml BSA, and 2 μM DTT] for 15 min at 37 C. The preincubated samples were mixed with 110 μl reaction buffer [0.1 M Tris-HCl (pH 7.5), 2 mM EDTA, 0.2 mM nicotinamide adenine dinucleotide phosphate reduced, and 0.4 U/ml yeast TRX reductase], and then 10 μl insulin solution [50 mM Tris-HCl (pH 7.5), 10 mg/ml insulin] were added to the mixture. The decrease in nicotinamide adenine dinucleotide phosphate reduced absorbance at 340 nm was recorded (maximal velocity, millioptical density at 340 nm/min) at room temperature. The calculated values were compared with the standard curve for recombinant TRX to obtain a quantitative determination of the absolute amounts of TRX.

Yeast two-hybrid analysis

The yeast two-hybrid analysis was performed using the yeast MATCHMAKER two-hybrid system (CLONTECH), according to the manufacturer's directions. *S. cerevisiae* strain AH109 transformed with pGBKT7-TLIMP or pGBKT7-TBP-2, together with either pACT2 or pACT2-TRX, respectively. Transformed colonies were cultured in synthetic medium with or without histidine.

Cell proliferation assay

Blasticidin-resistant mammalian expression vectors were introduced into CHO cells, and the cells were cultured with 8 μg/ml of blasticidin-containing medium for 2 or 3 d to eliminate the nonresistant cells. The blasticidin-resistant cells (3–5 × 10^3 cells in 100 μl of culture medium containing 8 μg/ml of blasticidin) were cultured in 96-well flat-bottom microtiter plates. Cell proliferation was measured as the formation of formazan using SF cell-counting reagents (Nacalai Tesque, Kyoto, Japan), according to the manufacturer's instructions.

Colony formation assay

Blasticidin-resistant mammalian expression vectors were introduced into HeLa S3 cells, and the cells were cultured with 4 μg/ml of blasticidin-containing medium for 3 d. The cells (1 × 10^6 cells) were plated in 0.35% agar containing DMEM, 10% FCS, and 4 μg/ml of blasticidin on a 0.5% agar base layer containing DMEM. The total number of foci was scored after 10 d.

Statistical methods

Results are expressed as means ± SD. Statistical comparisons were made using Student's *t* test or ANOVA coupled with a Fisher's test. A statistically significant difference was defined as $P < 0.05$, which is represented by an *asterisk* in the data presentation.

Results

TBP-2 protein family

As shown in Fig. 1A, BLAST searches were used to identify human genes homologous to TBP-2. DRH1 and two other genes (GenBank accession no. AF193051 and BC015928) were identified. DRH1 has been reported as a gene that is down-regulated in advanced human hepatocellular carcinoma (26). Here we refer to BC015928 as TLIMP, which was originally identified as KIAA1376 when it was found in the full-length human cDNA sequencing project (27). The function of AF193051 has not been reported. TLIMP has 40% identity and over 80% similarity with TBP-2 at the amino acid level, and the other genes also exhibit high levels of identity and similarity. All the genes included eight exons, each of which encodes a corresponding region of the protein (Fig. 1B and supplemental Fig. 1, published as supplemental data on The Endocrine Society's Journals Online web site at http://endo.endojournals.org). Therefore, it is likely that this mammalian gene family was generated by gene duplications. The members of the TBP-2 gene family also have some homology to arrestin proteins. For example, TLIMP has 25% similarity with β-arrestin-1 at the amino acid level. TBP-2 and arrestins have similar numbers of amino acids (~400) and show overall similarity, rather than just a highly conserved region.

TLIMP cDNA was cloned from a 293-cell cDNA library by PCR and then sequenced. Two isoforms of TLIMP cDNA with different lengths were found (Fig. 1C). The longer cDNA encoded full-length TLIMP, producing a protein of 414 amino acids. The shorter TLIMP splice variant, referred to as TLIMPs, lacks 148 bp corresponding to exon 3, generating a 24-amino-acid C-terminal tail and a translational stop codon and producing a shorter protein of 144 amino acids (Fig. 1D).

Tissue distribution of TLIMP expression

The expression of TLIMP was analyzed in normal human tissues and human cancer cell lines, and as shown in Fig. 2A, the size of TLIMP mRNA was about 4.5 kb in both normal and cancer cells. Strong expression of TLIMP was detected in normal skeletal muscle, placenta, kidney, adrenal gland, lymph node, mammary gland, thyroid, and trachea, but only very weak expression was detected in normal colon, thymus, spleen, small intestine, bladder, and bone marrow. In human cancer cell lines, TLIMP was strongly expressed in the lung adenocarcinoma cell line A549, whereas low expression levels were observed in other cancer cell lines. The expression of TBP-2 was strong in normal heart, skeletal muscle, spleen, and peripheral blood lymphocytes, and weak in normal brain and liver (Fig. 2B). The distribution of TLIMP was clearly different from that of TBP-2 in some tissues.

TLIMP does not interact with TRX

TBP-2 binds to TRX *in vivo* and *in vitro* (14), but no interaction of TLIMP with TRX was detected in a yeast two-hybrid analysis, as shown in Fig. 3A. The same analysis showed binding of TRX with TBP-2. Similar results were obtained in *in vitro* binding assays, in which TBP-2 coprecipitated with GST-TRX, but TLIMP failed to do so (Fig. 3B). Overexpres-